

De-scalping of the brain in echo planar DT-MRI

A. Purwar¹, R. Gupta², M. K. Sarma¹, G. Bayu¹, A. Singh¹, D. K. Rathore¹, S. Sakseena², R. Trivedi², A. Mishra², M. Haris², P. Mohan², R. Rathore¹

¹Mathematics, Indian Institute of Technology, Kanpur, UP, India, ²Radiodiagnosis, Sanjay Gandhi Post Graduate Institute of Medical Sciences, Lucknow, UP, India

Introduction: De-scalping in the brain is a very useful procedure with enormous applications in visualization, surface rendering, decreasing the complexity of subsequent processing algorithms, and the like. Many applications related to brain imaging either require, or benefits from the ability to accurately segment brain from the non-brain tissue. For example, (a) in the registration of b_0 -images to DW images in DT-MRI, both b_0 and DW images often contain considerable portions of eyeballs, skin etc. that cause problems in the registration process, which gets improved once these non-brain parts of the images are removed, (b) a second application of de-scalping is in tissue-type segmentation via DT-MRI, which helps in isolating brain tissue from other parts of the stack such as CSF, (c) in the removal of strong ghosting effects which can occur with EPI, (d) in visualization of DT-MR metrics, the dynamic range gets improved after de-scalping. This work describes an automatic procedure for de-scalping in the brain for echo planar MR images for scans with axial orientation.

Materials and Methods: The method takes entire image stack, removes the scalp and returns the stripped brain part. It works in two phases: In phase I, for each slice: (1) The averaged raw pixels (Fig 1a) are subjected to a negative quadratic exponential weighing $\exp(-\|x\|^2)$, (x denotes the pixel vector from the center of inertia of the image and the norm is induced by the elliptical inner product associated with an ellipse circumscribing the image) of the pixel intensities depending on the pixel position (Fig. 1b). (2) Above is followed by isoData threshold function (as in [3]) (Fig. 1c). This gives a binary mask (a very rough approximation of the brain) removing most of the background and darker pixels of the scalp (Fig. 1d). (3) Next this binary mask is subjected to a hole-filling (Fig. 1e) algorithm (as in [3]) which fills holes in 8-connected particles and also in child particles. (4) Above is followed by an opening operation (Fig. 1f, 1g) using a circular window of radius r ($r=2.0$) in order to remove connections around the eyes and ears. (5) Next each connected component in the mask obtained from step 4 is labeled (only those connected components are labeled which have number of pixels more than a threshold t ($t = 50$), the rest are put to zero assuming that they belong to the background) and grown upto p pixels ($p=80$) based on the SNR (SNR is computed based on the smoothed image intensities). In case of very low SNR, component is not grown. The growing procedure is iterative. This leaves a mask containing brain and some parts of the nose and eyes. Holes in this mask are further filled using a hole filling algorithm. This finishes phase I. Phase II: Masks for each slice obtained from phase I form stack mask. Firstly, the method fixes the slice orientation of the stack- mask from 'above to down' based on the number of connected components (note: at top level brain contains only one connected component) in each slice. This helps in removing the non-brain portions, e.g., eyes, nose etc. which are difficult to get rid of using the intensity alone. Now the method starts from above to downwards. It first finds out the center of inertia (based on the position and raw pixel intensities) of a slice and for each connected component in following slice. Now the Euclidian – distance between the centers of inertia of each connected component in the slice under consideration and upper slice is computed. Those connected components of the slice are preserved which have distance less than a distance-threshold (in our experiments, for 256×256 images distance-threshold is 60 pixels and is proportional to the size of images in general). This removes the eye balls (Fig. 1h). Above is followed by a dilation and then a erosion operation via finding minimum and maximum over a circular window of radius r ($r = 2.0$) respectively in both the sagittal and coronal views in-order to remove nose and ear portions (Fig. 1i). This completes phase II. The current method is implemented using JAVA programming language at the Advanced Digital Imaging Solutions Laboratory (ADISL) at IIT Kanpur [4].

To test the procedure whole brain diffusion tensor MRI data for fifteen healthy volunteers was acquired on a 1.5 Tesla GE MRI scanner at the SGPGIMS, Lucknow using single-shot echo planar dual spin-echo sequence with ramp sampling. The diffusion weighting b-factor was set to $1000s/mm^2$, TR~8sec, TE~100ms. A total of 21-34 axial sections were acquired with a slice thickness of 3mm, no gap, FOV= 240 mm x 240 mm and an image matrix of 256×256 (following zero filling). The diffusion tensor encoding used was the balanced, rotationally invariant icosahedral/dodecahedral scheme with 21/10 uniform directions over the unit hemisphere. The procedure was tested on the b_0 stack of each DT-MRI data set. Results were visually inspected and compared with the Brain Extraction Tool (BET) implemented in MRI-cro interface version 1.39.

Results: The method is found to be encouraging and produces good results. Data surfaces in all the cases were computed using the freely available MRI-cro interface version 1.39. Before computing surfaces a voxel interpolation was performed using cubic B-spline.

Figure 2 shows (best at 500% resolution) the overlaid brain boundary obtained from the current method (red color) and BET (green color) onto the entire raw stack. Here yellow color shows the intersecting boundary. The images clearly show that the BET procedure (at fractional intensity 0.50, which we found best for our images) overdoes the de-scalping by removing a significant part of the brain. On the other hand the stripped image from the current method does not suffer from this defect. In Figure 3(a) and 3(b) the first, second and third columns show the axial, sagittal and coronal view of the surfaces obtained from BET and the current method as we move

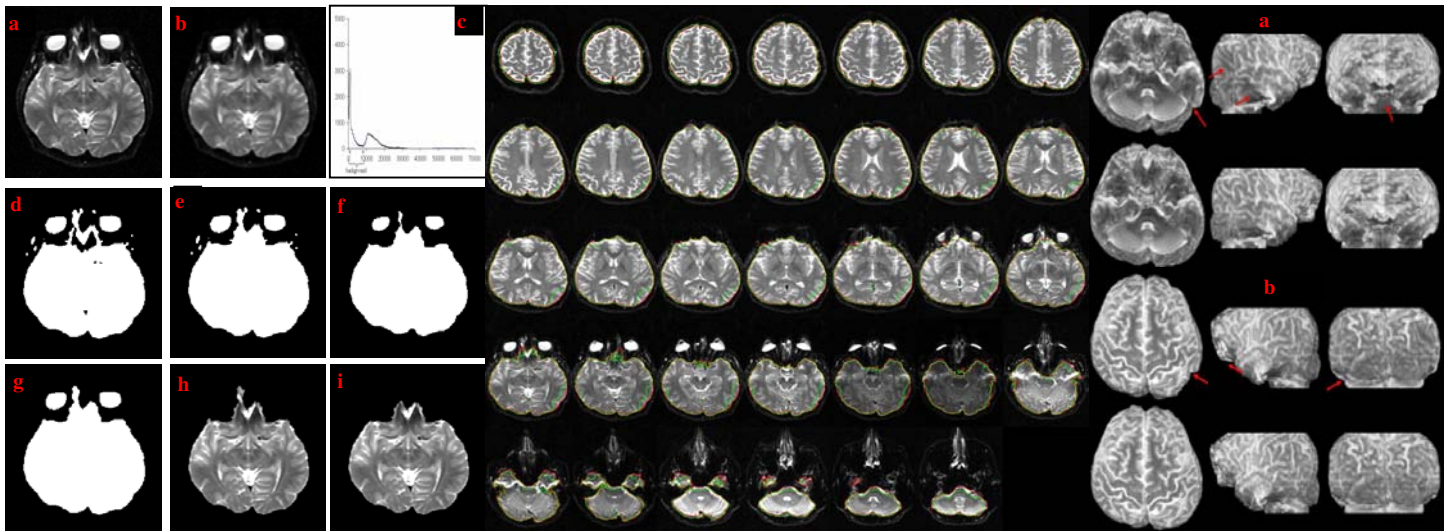


Figure 1

Figure 2

Figure 3

from downward to above and above to downward respectively. Arrows in both the images clearly show the differences in BET and the proposed method.

Discussion: Experiments with the method did result in good extractions. However in some cases of T2 hyperintense globe in the orbital region it failed to remove this structure. Fortunately, in such cases these extra parts are well separated from the main brain allowing a removal by a conventional paint-brush without much effort.

References: [1] Stephen M. Smith, Fast Robust Automatic Brain Extraction, Hum Brain Mapp. 2002 Nov;17(3):143-55. [2] <http://www.cla.sc.edu/psyc/faculty/rorden/micro.html>. [3] ImageJ: <http://rsb.info.nih.gov/ij/>. [4] DT-MRI Computation Manual, ADISL, IIT Kanpur, 2005.